Environ. Sci. Technol. **2007**, *41,* 4332−4338

Relevance of Nontoxigenic Strains as Surrogates for *Escherichia coli* O157:H7 in Groundwater Contamination Potential: Role of Temperature and Cell Acclimation Time

FELIPE D. CASTRO AND NATHALIE TUFENKJI*

Department of Chemical Engineering, McGill University, Montreal, Quebec H3A 2B2, Canada

Nontoxigenic bacteria are commonly used as indicators for predicting the contamination potential of pathogens in natural or engineered aqueous environments. In this study, column transport experiments were used to examine the relevance of two nontoxigenic strains of *Escherichia coli* O157:H7 as potential surrogates for the well-known pathogen. Experiments conducted at 11 °C indicate that only one of the nontoxigenic strains may be an appropriate surrogate for predicting the migration potential of the pathogen at low solution ionic strengths. Results of various bacterial characterization methods indicate that differences in cell attachment could qualitatively, but convincingly, be related to differences in cell surface charge. Additional experiments conducted at 22 °C reveal the influence of temperature on bacterial cell surface charge and cell attachment to sand. The role of cell acclimation time to an artificial groundwater solution is also examined, showing little change in the degree of cell attachment over a period of several weeks.

Introduction

The contamination of drinking water by microbial pathogens is recognized as one of the most pressing water supply problems of our day. Two important sources of pathogen contamination are animal fecal deposits associated with intensive livestock production and manure spreading in agricultural applications. Smith and Perdek (*1*) list several examples of manure-related waterborne disease outbreaks that have occurred in the U.S., U.K, Canada, and Japan. A number of these cases involved the bacterium *Escherichia coli* O157:H7—an enterohemorrhagic organism producing Shiga-like toxins that can cause severe bloody diarrhea and abdominal cramps (*2*). In May 2000, in Walkerton, Ontario, 2300 people were infected with *E. coli* O157:H7, and several individuals were also co-infected with *Campylobacter jejuni* (*1*, *3*). Seven people died as a result of this outbreak, which was linked to the infiltration of bacteria from cow manure into the aquifer supplying the municipal well water (*3*).

Although agricultural waste disposal near potable water supplies has been linked with outbreaks of disease, the physical, chemical, and biological factors controlling pathogen filtration in the complex subsurface environment are not well-understood. Moreover, few systematic studies have been conducted to evaluate the retention of pathogens in such environments. In general, transport of disease-causing microorganisms in granular media has been investigated using surrogate particles or organisms (*4*, *5*). For instance, many studies of bacterial transport in soils or sands have been conducted with nonpathogens (*6*, *7*). As a result, little is known regarding the transport properties of toxigenic microorganisms, such as *E. coli* O157:H7. The few laboratory studies that have reported on the transport behavior of this waterborne pathogen have used nonpathogenic strains of the same serotype, rather than the infectious strain (*8*−*10*). Morrow et al. (*9*) examined the transport of a nontoxigenic *E. coli* O157:H7 (ATCC 700728) in columns packed with five different minerals. Results of this work show that 700728 binds strongly to Pyrax; however, the relevance of this finding for the disease-causing *E. coli* O157:H7 has not been confirmed.

The objective of this study is to evaluate the relevance of nontoxigenic strains of *E. coli* O157:H7 as potential surrogates for the subsurface transport of the pathogen. Sand-packed columns are used to study the migration of two nontoxigenic strains and one pathogenic strain of *E. coli* O157:H7 over a range of solution ionic strengths (IS). Experiments conducted at two temperatures provide insight into the influence of this environmental parameter on bacterial transport in saturated porous media. In addition, the effect of cell acclimation time to an electrolyte solution is examined for time periods ranging from 18 h to 21 days.

Materials and Methods

Bacterial Cell Preparation and Characterization. Three strains of *E. coli* O157:H7 were used in this research. ATCC 700728 and 43888 are nontoxigenic strains lacking the genes encoding for Shiga-like toxins I and II. ATCC 700927 (more commonly known as EDL933) is positive for both Shiga-like toxins, and its complete genome has been sequenced (*11*).

Pure cultures were maintained at −80 °C in Luria−Bertani Lennox broth (25 g/L) (Fisher) with 15% glycerol. One week prior to experimentation, cultures were streaked onto LB agar plates that were then incubated at 37 °C for 24 h. For each experiment, a single colony from a fresh plate was used to inoculate 150 mL of LB broth (in a 500 mL baffled flask). The culture was incubated at 37 °C for 8 h at 200 rpm to an early stationary phase at which point the cells were harvested. This growth protocol did not result in expression of the virulence factors in enteropathogenic *E. coli* (*12*). The bacterial suspension was centrifuged (Sorvall RC6) for 15 min at 5860*g* in an SS-34 rotor (Kendro). The growth medium was decanted, and the pellet was resuspended in an electrolyte (0.01, 0.05, 0.1, 1, or 10 mM KCl). To remove all traces of the growth medium, the cells were centrifuged and resuspended in fresh electrolyte one additional time. Washed cells suspended in KCl (~4×10^9 cells/mL) were then incubated at 10 °C for 18 h. This incubation at cold temperature was used to replicate conditions that may be encountered by cells following release into groundwater representative of the Canadian climate. Prior to conducting transport experiments, cells were diluted in the appropriate electrolyte (at 10 °C) to the desired final concentration of ~4×10^7 cells/mL. The pH of the suspensions was adjusted to 5.7−5.9 using 0.1 M HCl if needed. Analytical reagent-grade KCl and HCl (Fisher) and deionized (Milli-Q) water were used to prepare electrolytes.

* Corresponding author phone: (514) 398-2999; fax: (514) 398-6678; e-mail: nathalie.tufenkji@mcgill.ca.

10.1021/es0701558 CCC: $37.00
Published on Web 05/18/2007

Plate counts were used to verify loss of cell viability during incubation in the electrolyte at 10 °C. Cell suspensions were diluted in High Recovery Diluent (Oxoid), spread plated on R2A agar (Difco; in triplicate), and incubated for 24 h (37 °C) before counting. Cell viability for ATCC 700728, 700927, and 43888 was found to be greater than 87% over the range of IS.

The nominal size of the bacteria was determined using two approaches: (i) by dynamic light scattering (DLS) (Zetasizer Nano ZS, Malvern) and (ii) by analyzing images taken in an inverted fluorescent microscope operating in phase contrast mode. In this latter approach, an image processing program (ImageJ, NIH) was used to determine the average lengths of the major and minor axes of the cells, and the resulting equivalent spherical diameter was compared to that obtained by DLS.

Microelectrophoresis (ZetaSizer Nano ZS, Malvern) was used to characterize the electrokinetic properties of the cells over the range of IS used in the experiments. Electrophoretic mobility (EPM) was measured at 11 °C using cell suspensions ($\sim 4 \times 10^7$ cells/mL) prepared in the electrolyte of interest. These measurements were repeated using at least three different samples of each bacterial suspension.

Relative cell surface hydrophobicity was evaluated by contact angle measurements (sessile drop technique) on bacterial lawns formed on a cellulose acetate membrane filter (0.45 μm, 47 mm diameter, GE Osmonics) using the method described in ref *13*. At least four measurements were made on each filter, and at least three filters were used for each condition. Because of equipment limitations, electrolyte contact angles were measured at 22 °C rather than the temperature of the transport experiments (11 °C). Although the temperature has been shown to have an effect on contact angle measurements (*14*), the data obtained at 22 °C were deemed adequate for qualitative comparison between the three strains.

Potentiometric titrations were conducted to determine the pK_a values and proton binding site concentrations (S_i) of macromolecules located on the bacterial surface. Bacterial suspensions prepared in 10 mM KCl (7.5×10^9 to 1.1×10^{10} cells/mL, 11 °C) were purged with N_2 gas in a closed vessel and then adjusted to pH 4 with 0.1 N HCl, and titrations were conducted to pH 11 using 0.1 N NaOH (798 Titrino, Brinkmann Metrohm). Titrations were repeated at least twice. The pK_a values of ionizable functional groups on the cell surface and corresponding concentrations of these groups (S_i) were evaluated using the chemical speciation software FITEQL 4.0 as previously shown (*15*, *16*).

Porous Media Preparation and Characterization. High purity (99.76% SiO_2) quartz sand (Granusil #2040, Ottawa Plant, Unimin) was utilized as model granular media. The sand was size fractioned with nylon sieves (U.S. standard mesh sizes 20 and 25) and thoroughly cleaned to remove impurities (*17*). The cleaning steps included soaking the sand in 12 N HCl for 20 h, washing in deionized water, repeating the acid soak and water rinse step, and baking at 800 °C for 6 h. Cleaned sand was stored in a dry glass bottle and rehydrated by soaking in the electrolyte of interest for 18 h (at 10 °C) before packing the column. Microscopic examination of the sand grains revealed them to be well-rounded, and standard sieve analysis yielded an average grain diameter (d_{50}) of 0.763 mm. The point of zero charge of quartz is ~pH 2; hence, the overall charge on the sand grains is negative at the pH of the experiments.

Bacterial Transport and Deposition Experiments. Column experiments were conducted to evaluate the transport of the three *E. coli* O157:H7 strains separately under fully saturated conditions. The experimental apparatus was placed inside a cold chamber maintained at 11 °C. Preparing cell suspensions and granular media at a slightly colder temperature (10 °C) facilitated conducting the experiment at

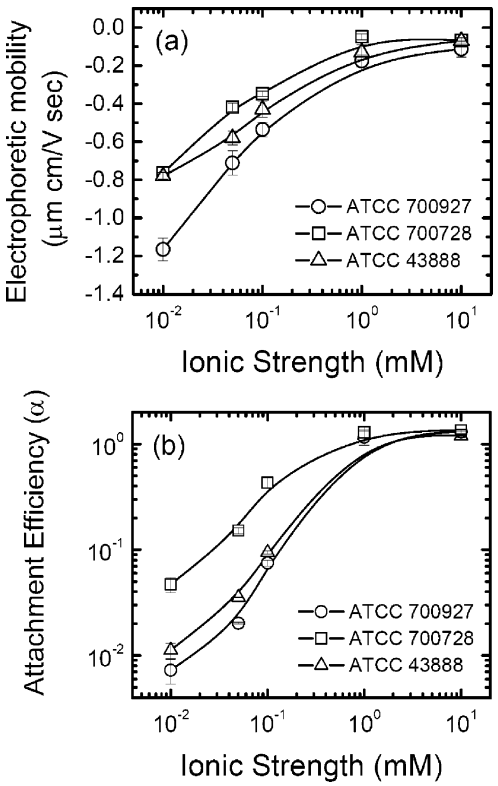

FIGURE 1. (a) Electrophoretic mobility of (○) ATCC 700927; (□) ATCC 700728; and (Δ) ATCC 43888 over a range of IS (KCl). (b) Attachment efficiencies (α) calculated using eq 1 and results from bacterial breakthrough curves (Figure S1) for (○) ATCC 700927; (□) ATCC 700728; and (Δ) ATCC 43888 as a function of IS. Key experimental conditions were approach velocity = 1.7×10^{-4} cm/s, porosity = 0.35, mean grain diameter = 0.763 mm, pH = 5.7−5.9, and temperature = 11 °C.

11 °C (due to a slight heat gain by these materials during transfer to the chamber). Experiments were conducted by pumping a bacterial suspension through a glass column packed with clean saturated sand. An adjustable height column (C 10/40, Amersham) with an inner diameter of 1.0 cm was used. The sand was wet-packed to a height between 89 and 298 mm with vibration. Standard gravimetric methods were used to determine the sand density (2.62 g/cm^3) and a column packing porosity of 0.35.

Prior to each experiment, the packed column was equilibrated by injecting (Model 200 syringe pump, KD Scientific) 20 pore volumes (PV) of the background electrolyte solution through the column at an approach velocity of 1.7×10^{-4} cm/s. A bacterial suspension of concentration (C_0) 4×10^7 cells/mL and of the same background electrolyte composition was pumped for at least 4 PV followed by a bacteria-free electrolyte solution (4 PV). The bacterial cell concentration at the column outlet was monitored on-line with a UV−vis spectrophotometer (Hewlett-Packard Model 8453) and a 1 cm flow-through cell (at 600 nm). Each experiment was conducted at least twice, and very good reproducibility was observed.

Results and Discussion

Characterization of Bacterial Cells. In Figure 1a, EPMs of the two nontoxigenic strains of *E. coli* O157:H7 (43888 and 700728) and the toxigenic strain (700927) are presented as a function of solution IS. All three strains of *E. coli* O157:H7 are negatively charged over the range of salt concentrations examined, as commonly observed for bacteria suspended in aqueous media (*18*). Figure 1a also shows that the EPM becomes less negative with increasing IS. This behavior can

be attributed to the compression of the electrical double layer as a result of increasing concentration of potassium ions. Strain 700728 exhibits the lowest absolute charge over the range of IS, whereas the toxigenic 700927 is more negatively charged. The measured EPM for 43888 is in between the values observed for the two other strains. *E. coli* O157:H7 EPM measured here may not be directly compared to previously reported values (*9*, *19*, *20*) as cell growth, handling, and measurement techniques vary in each study, and it is known that differences in cell preparation protocols can influence the determination of cell surface properties (*21*). Nonetheless, the EPMs measured here for *E. coli* O157:H7 are within the range of values previously reported (*8*, *9*, *20*).

The negative charge of bacterial cells is linked to the nature of macromolecules in the outer cell wall (e.g., proteins and complex lipids) (*15*, *18*). Ionizable functional groups that make up these macromolecules (e.g., amine, carboxylic, phosphoric, and hydroxyl groups) control the nature of the cell surface charge under different conditions. Hence, differences in the chemical composition of cell walls for the three strains could explain the observed variability in the cell EPM. Although the bacteria used in this study are all *E. coli* of the same serotype, 700728 and 43888 are not controlled knockout mutants of EDL933 (i.e., the nontoxigenic strains may be missing more genes than those encoding the Shiga-like toxins, such as genes encoding for membrane bound proteins). A comparison of pK_a values and proton binding site concentrations (S_i) determined from potentiometric titrations conducted on the three strains at 11 °C is presented in Table 1. The best fit of the experimental data was obtained using four pK_a values in FITEQL 4.0, which is in agreement with previous studies (*15*, *22*). The first three pK_a values are similar for all three strains ($pK_{1,avg} = 4.11$ is likely associated with carboxylic and/or phosphoric groups; $pK_{2,avg} = 5.86$ is likely associated with the carboxylic group; and $pK_{3,avg} = 7.82$ is likely associated with the phosphoric group), whereas pK_4 (likely associated with amine or hydroxyl groups) changes slightly between each strain (Table 1) (*15*). The concentrations of proton binding sites (S_i) are also fairly consistent, with the exception of some differences in S_2 and S_4. These measured variations in charging properties of the different strains are an indication of differences in the quantity and/or type of biomolecules at the cell surfaces.

Contact angle measurements on bacterial lawns are commonly used to characterize the relative hydrophobicity of cell surfaces (*13*, *23*). Results of contact angle measurements on lawns of the three *E. coli* O157:H7 strains are presented in Table 1 for two KCl concentrations. Measurements were done using the same electrolyte in which the cells had previously been incubated. The results indicate that there is no observable difference in the measured contact angles between the three bacteria.

Also included in Table 1 is the average equivalent spherical diameter of the three strains determined by DLS over the range of IS investigated. These measurements reveal no significant differences in the average size of the three *E. coli* strains, and there is no observable change in cell size with IS. Measurements of equivalent cell diameter determined by analysis of microscope images are smaller than those determined by DLS (Table 1); however, the average measured length of the major axis is close to the cell size determined by DLS (data not shown).

Transport of *E. coli* O157:H7 in Saturated Granular Media. Breakthrough curves obtained from column experiments conducted with the three *E. coli* strains are provided in the Supporting Information (Figure S1). The transport behavior of each bacterium was examined over a broad range of IS at 11 °C. The attachment efficiency, α, from colloid filtration theory can be used to quantitatively compare the extent of bacterial attachment observed for the different

TABLE 1. Summary of Measured Cell Properties for Three Strains of *E. coli* O157:H7

strain	η_0[d]	contact angle[a]		cell size by DLS and microscopy[b]				dissociation constants and site concentrations[c]									
		0.1 mM	10 mM	0.01 mM	0.1 mM	1 mM	10 mM	pK_1	S_1	pK_2	S_2	pK_3	S_3	pK_4	S_4
ATCC 700927[e]	1.7×10^{-3}	21.6 ± 0.5	20.6 ± 1.1	1355 ± 206	1286 ± 250	1355 ± 21	1380 ± 209	4.15 ± 0.06	46.2 ± 3.5	5.86 ± 0.03	36.2 ± 2.1	7.87 ± 0.01	41.5 ± 2.8	10.31 ± 0.08	61.7 ± 3.7
	2.0×10^{-3}			*1419 ± 90*	*1613 ± 115*	*1515 ± 66*	*1470 ± 154*	*3.99 ± 0.14*	*65.6 ± 12*	*5.88 ± 0.08*	*43.8 ± 7.2*	*7.70 ± 0.09*	*44.3 ± 1.2*	*10.55 ± 0.29*	*162.8 ± 51*
				(740)	(760)	(700)	(740)								
ATCC 700728	1.7×10^{-3}	21.8 ± 1.4	23.0 ± 0.9	1317 ± 173	1304 ± 233	1350 ± 184	1450 ± 324	4.14 ± 0.13	46.3 ± 2.3	5.82 ± 0.07	35.8 ± 0.4	7.77 ± 0.11	39.8 ± 0.4	10.47 ± 0.08	77.1 ± 3.3
	2.0×10^{-3}			*1525 ± 134*	*1633 ± 33*	*1588 ± 68*	*1673 ± 124*	*3.99 ± 0.09*	*65.2 ± 7.6*	*5.94 ± 0.06*	*39.8 ± 1.8*	*7.90 ± 0.13*	*39.5 ± 0.7*	*10.96 ± 0.14*	*256.7 ± 40*
				(740)	(710)	(720)	(730)								
ATCC 43888	1.6×10^{-3}	21.8 ± 1.3	21.4 ± 3.1	1300 ± 150	1446 ± 153	1440 ± 57	1524 ± 38	4.04 ± 0.02	50.1 ± 2.6	5.91 ± 0.04	30.7 ± 0.3	7.83 ± 0.05	44.1 ± 1.1	10.64 ± 0.02	90.0 ± 0.6
				(710)	(740)	(700)	(760)								

[a] Measured at room temperature (22 °C) using KCl solutions of two different ionic strengths as indicated; reported as average ± standard deviation. [b] Equivalent spherical diameter (in nm) of the bacterial cells as evaluated by DLS and microscopy; reported as average ± standard deviation. Values in italics were determined at 22 °C. Values in parentheses were determined by microscopy. [c] pK_a values and proton binding site concentrations (S_i) are determined from results of potentiometric titrations conducted with each strain in 10 mM KCl (using FITEQL 4.0). Values in italics were determined at 22 °C. [d] Values of η_0 are calculated using eq 17 in ref *24* using the overall average cell diameter (d_p) determined by DLS for each strain, average grain diameter (d_c) of 0.763 mm, water viscosity and density at the respective temperatures, a value of 6.5×10^{-21} J/K for the Hamaker constant of bacteria, a particle density (ρ_p) of 1.050 g/cm^3 for bacteria, and a packed-bed porosity (ϵ) of 0.35. Values in italics are for conditions at 22 °C. [e] toxin producer.

strains at various solution IS (*24*, *25*). The attachment efficiency is a dimensionless deposition rate evaluated as the ratio of the single collector removal efficiency (η) and the theoretical single collector contact efficiency (η_0) that can be determined by a numerical solution of the convective diffusion equation or a correlation equation (*24*). The attachment efficiency, α, was calculated from each breakthrough curve as follows:

$$\alpha = -\frac{2}{3}\frac{d_c}{(1-\epsilon)L\eta_0}\ln(C/C_0) \quad (1)$$

where d_c is the diameter of the sand grains, ϵ is the bed porosity, and L is the bed length (*25*). The value of C/C_0 in eq 1 was obtained from each breakthrough curve (Figure S1) by averaging values measured between pore volumes 1.9 and 2.1. Values of η_0 for these experimental conditions (Table 1) were determined using a correlation developed by Tufenkji and Elimelech (*24*). Calculated α values for the three *E. coli* strains are plotted in Figure 1b as a function of IS. For all three strains, the attachment efficiency increases with increasing IS (in qualitative agreement with the Derjaguin−Landau−Verwey−Overbeek (DLVO) theory of colloidal stability (*26*, *27*)); however, there is a critical salt concentration (about 1 mM KCl) where α reaches a value near unity and an increase in IS does not result in higher deposition rates (i.e., the bacterial deposition rate has reached the maximum transport limited rate).

Figure 1b reveals that the three strains exhibit different attachment efficiencies to the quartz sand (note logarithmic scale) at lower IS. The nontoxigenic 700728 has the highest α values over the range of IS investigated, whereas the toxigenic 700927 has the lowest degree of retention in the column. Attachment efficiencies evaluated for the nontoxigenic 43888 are in between those determined for the two other strains but quite close to those measured for 700927. Both of the nontoxigenic organisms attach to a greater extent to the sand than the toxigenic *E. coli*. This finding has important implications for the selection and use of such nontoxigenic mutants as surrogates for their toxigenic counterparts. Indicators should be chosen on the basis that they exhibit less attachment to subsurface granular media than pathogens. These results clearly show that the nontoxigenic 700728 is not a relevant indicator for *E. coli* O157:H7, whereas 43888 can be considered a better surrogate.

To explain the observed trends in Figure 1b, we should consider the physical and physicochemical properties of the three strains. Variations in cell size may give rise to different microbe removal mechanisms (e.g., physical straining) (*28*); however, no significant variation in cell size was observed over the range of conditions investigated (Table 1), suggesting that this cell property cannot account for the observed differences in bacterial removal. Some studies have shown that cell hydrophobicity can influence bacterial attachment to surfaces (*13*, *29*); however, examination of cell surface hydrophobicity via contact angle measurements did not reveal any significant differences between the strains (Table 1), indicating that this cell property is not the main cause of the observed differences in α. Comparison of α values and EPMs (Figure 1) indicates that bacterial attachment increases with decreasing absolute EPM. Calculated attachment efficiencies mirror the trends in EPM whereby the least charged strain exhibits the greatest degree of attachment and the most highly charged strain presents the lowest α values. These trends in α are in qualitative agreement with the DLVO theory of colloid stability for unfavorable (i.e., repulsive) colloidal interactions (*30*).

Applying the DLVO theory to our system, variations in the magnitude of the bacteria−sand surface interaction energies will depend mainly on the bacteria cell surface (zeta

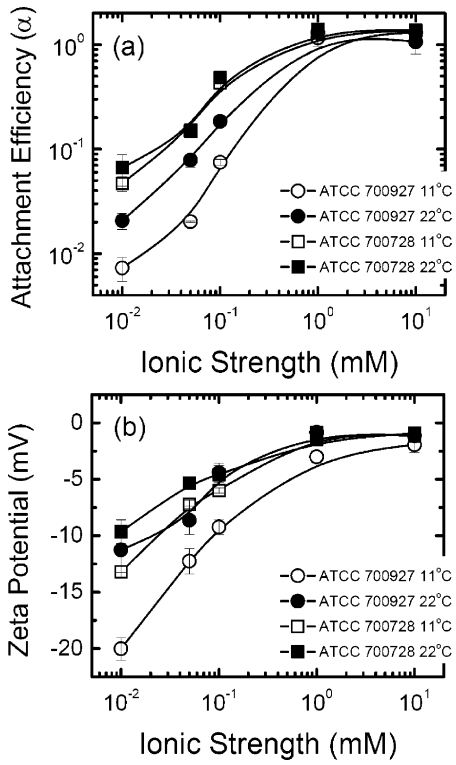

FIGURE 2. (a) Attachment efficiencies (α) calculated using eq 1 for ATCC 700927 (toxin producer) and ATCC 700728 at temperatures of 11 °C (open symbols) and 22 °C (solid symbols) as a function of IS. (b) ζ potentials of ATCC 700927 and ATCC 700728 at 11 °C (open symbols) and 22 °C (solid symbols) over a range of IS. Other experimental conditions were the same as in Figure 1.

(ζ)) potential (since all other parameters such as sand grain ζ potential, cell size, and temperature are approximately constant at a given IS). On the basis of DLVO theory, cells with a greater absolute potential are expected to experience a greater repulsive force upon approach to the sand surface in comparison to cells exhibiting a lower surface potential. This explains (i) the greater degree of attachment observed with increasing IS for all three strains (due to double layer compression) and (ii) the variation in attachment observed between the three strains at lower IS (in agreement with measured differences in EPM).

Role of Temperature in Bacterial Deposition. Most laboratory studies of colloid or microbe transport in granular media have been conducted at room temperature (e.g., refs *31* and *32*). In the previous section, we report results of experiments conducted at a lower temperature representative of average groundwater temperatures in Canada and the northern U.S. (*33*). To better understand the influence of temperature on bacterial transport in granular media, an additional set of experiments was carried out with 700927 and 700728 at room temperature (22 °C). Cells were cultured and harvested as described previously, except for cell acclimation in electrolyte that was conducted for 17.5 h at 10 °C, then at 22 °C for 30 min. Cell sizes measured for bacteria conditioned to 22 °C are slightly larger than those maintained and measured at 11 °C (Table 1).

Attachment efficiencies of strains 700927 and 700728 evaluated at 22 °C are compared to those determined at 11 °C in Figure 2a. Comparison of α values determined at different temperatures is possible since the influence of temperature on physical system properties (e.g., fluid viscosity, fluid density, etc.) is taken into account in η_0 (*24*). The data presented in Figure 2a show that 700927 generally exhibits a higher degree of attachment at the higher tem-

perature. In contrast, α values determined for 700728 are similar at the two temperatures. These results are significant with respect to the use of these nontoxigenic microbes as indicators for the pathogen as well as the design of laboratory experiments for the prediction of pathogen migration in groundwater. The comparison shown in Figure 2a reveals that conducting column experiments at room temperature is generally not appropriate for extrapolation to field conditions. For the case of 700927, if studies were conducted only at room temperature, the migration potential of this pathogen in groundwater would be significantly underestimated. Furthermore, the data show that if experiments were carried out only with the nontoxigenic strain, the potential influence of temperature on attachment may not be recognized.

Electrokinetic properties for the two *E. coli* O157:H7 strains at the two temperatures of interest are presented in Figure 2b. ζ potentials calculated from the measured EPMs (using the Smoluchowski equation) take into consideration changes in solvent viscosity and dielectric constant with temperature (*34*). Overall trends in the ζ potential (Figure 2b) are generally in qualitative agreement with the bacterial attachment behavior (Figure 2a). Absolute values of the ζ potential for 700927 determined at 11 °C are greater than those at 22 °C over the range of IS investigated (in agreement with lower α values at 11 °C). A comparable trend in the ζ potential is observed for 700728, although the differences in cell charge at the two temperatures are not as large, and consequently, α values for this strain are fairly comparable at the two temperatures.

Few studies have examined the influence of temperature on cell or particle ζ potential (*14*, *35*). Gallardo-Moreno et al. (*14*) also observed a decrease in absolute ζ potential with increasing temperature (22−37 °C) for cells of *Enterococcus faecalis* but did not discuss the underlying cause of this behavior. To better understand the observed variations in ζ potential with temperature, our data for the two *E. coli* are compared to measurements obtained using silica (0.3 μm diameter, Nissan Chemical) and polystyrene latex colloids (1.5 μm diameter, Interfacial Dynamics) under identical conditions. The scaled electrophoretic mobility (M) and the scaled reciprocal double layer thickness (κa) are useful parameters that account for differences in particle size and solvent properties at the two temperatures investigated (*36*)

$$M = \left(\frac{V}{E}\right)\frac{3\eta_S e}{2\epsilon_S\epsilon_0 k_B T} \tag{2}$$

and

$$\kappa = \left[\frac{2000(\mathrm{IS})N_A e^2}{k_B T\epsilon_0\epsilon_S}\right]^{1/2} \tag{3}$$

where V is the velocity of a particle in the presence of an applied electric field E, η_S is the electrolyte viscosity, e is the elementary charge, N_A is Avogadro's constant, ϵ_0 and ϵ_S are the permittivity of a vacuum and dielectric constant of the electrolyte, a is the particle radius, k_B is Boltzmann's constant, and T is absolute temperature. In Figure 3, the scaled mobility is plotted as a function of κa for 700927 and 700728, the silica colloid and the latex colloid. For both nonbiological colloids, the data points determined at 11 °C are very similar to those evaluated at 22 °C, suggesting that there is no significant change in the physicochemical properties of the colloids (Figure 3a). However, for both bacteria, there is a gap in the data sets obtained at the two temperatures (i.e., the data do not collapse onto the same curve for a given cell type).

The observed difference in M at two temperatures for the bacteria may be partly attributed to changes in the degree of deprotonation of functional groups present in cell surface

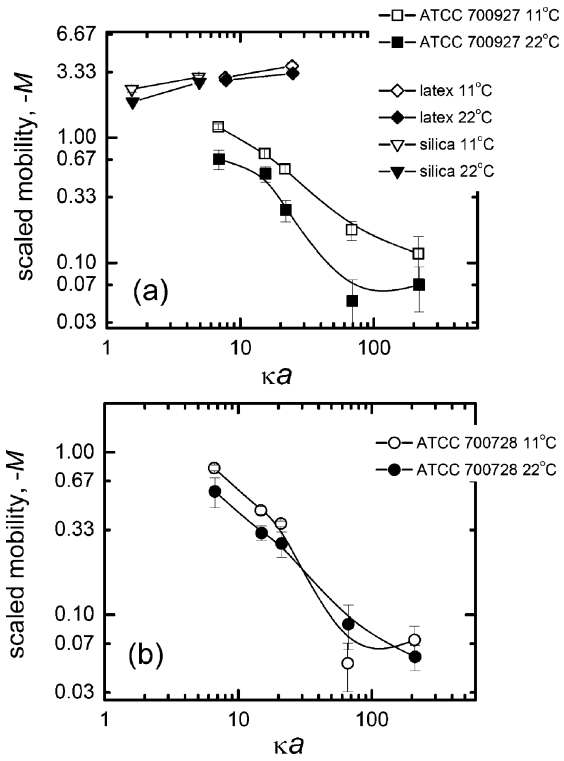

FIGURE 3. (a) Scaled electrophoretic mobility *M* as a function of the scaled reciprocal double layer thickness κa for latex particles, silica particles, and ATCC 700927 at 11 °C (open symbols) and 22 °C (solid symbols). (b) Scaled electrophoretic mobility *M* as a function of the scaled reciprocal double layer thickness κa for ATCC 700728 at 11 °C (open symbols) and 22 °C (solid symbols).

proteins or complex lipids. The dissociation constant of certain acidic and basic groups can vary with temperature (e.g., $-NH_3^+$), whereas the pK_a values of some functional groups are relatively insensitive to temperature (e.g., −COOH) (*37*, *38*). Variations in the extent of deprotonation of functional groups present at the cell surface could contribute to differences in the cell ζ potential. Cell titrations were repeated for the two bacteria at 22 °C, and fitted pK_a values and site concentrations (S_i) are included in Table 1. The results show slight variations in values of pK_4 for both strains between 11 and 22 °C. Differences are also observed in fitted values of S_1 and S_4. These changes in the concentrations of proton binding sites with an increase in temperature may be related to physiological properties of the bacterial cells (e.g., protein expression).

Another factor that may contribute to differences in M is a change in the degree of compression of cell surface polymers. Numerical solutions of the full electrokinetic model for soft spheres show that M decreases with increasing layer thickness of neutral polymers, whereas for thin coatings of charged polymer, M increases with layer thickness (*36*). Because temperature changes can influence the degree of compression of polymer coatings on cells, this may explain the observed changes in M when the temperature was increased. However, due to the inherent heterogeneity in the chemical composition and the amount of biomolecules present on cell surfaces, it is not straightforward to predict the response (i.e., conformational changes) of these cell surface polymers to changes in temperature. For example, some studies show small increases in protein size with temperature (*39*, *40*), whereas for amphiphilic poly(ethylene glycol) chains, a large increase in temperature (2−25 °C) resulted in a slightly thinner brush layer (*41*). Furthermore, because cells are coated with both charged and uncharged

macromolecules, it becomes more difficult to predict the effect of brush layer compression on *M*. In the present discussion, we have focused on changes in physicochemical cell properties with temperature. Temperature changes will also influence several physiological properties of cells, including membrane fluidity, surface hydrophobicity, and gene expression (*42*−*44*). In reality, several of these factors can play a combined role on the observed variations in *M* with temperature.

Migration of *E. coli* O157:H7 Following Extended Acclimation. Others have shown how cell growth or manipulation protocols can influence bacterial properties and attachment to surfaces (*14*, *21*, *45*, *46*). Here, we conducted experiments to investigate the influence of cell acclimation time on bacterial transport. Washed cell stock suspensions ($\sim 4 \times 10^9$ cells/mL) of strains 700927 and 700728 were incubated at 10 °C in 0.1 mM KCl, and samples were taken at specific times (18, 66, 162, and 522 h) and diluted (4×10^7 cells/mL) in 0.1 mM KCl prior to conducting column experiments (at 11 °C). Cell size, EPM, and viability were monitored for each experiment (Supporting Information, Table S1). No significant changes in cell size or EPM were observed over the 522 h period, and cell viability was quite high. Interestingly, attachment efficiencies for the two strains reached a relatively stable similar value following extended exposure to the nutrient-deprived environment. For 700927, α was 0.075 at 18 h and increased to 0.22 at 522 h, and for 700728, α decreased from 0.43 at 18 h to 0.20 at 522 h. Further studies are needed, however, to better understand and predict the transport of these pathogens in groundwater of varying nutrient and contamination levels.

Environmental Implications

The results of this study reveal insights on the selection and relevance of indicator organisms as surrogates for pathogens. To our knowledge, the transport and attachment behavior of toxigenic *E. coli* O157:H7 in granular systems has not been previously reported. Furthermore, few studies have been conducted that compare the transport of nonpathogens with that of pathogens in natural or model groundwater. Our findings show how nontoxigenic strains are not necessarily good surrogates for toxin producing bacteria, even when they are of the same serotype. For instance, on the basis of α values measured in 0.1 mM KCl (11 °C, Figure 2a) and eq 1, 5 m of travel distance is required to achieve 99% removal of the nontoxigenic 700728 from the pore fluid. In contrast, 29 m of travel is needed to achieve the same degree of removal for the pathogen (700927). It should be noted that the observed differences in retention of a pathogen versus a nonpathogen may fall within strain variation and may not be intrinsic to the difference between pathogens and nonpathogens as such. Further studies using well-controlled knockout mutants can provide additional insight into these differences in attachment behavior.

The experiments presented here were conducted in simple low IS electrolytes and clean quartz sand, whereas natural groundwater can contain a wide range of monovalent and multivalent salts, humics, and various (in)organics. The low IS examined here may be most relevant to conditions following rainfall events. Continuing research in our laboratory aims at extending this work to examine the transport of pathogens in natural agricultural soils over a broader range of environmentally relevant conditions. A better understanding of pathogen transport in the subsurface will lead to safer recommendations for agricultural waste disposal near recreational and drinking water supplies.

Acknowledgments

This research was supported by NSERC (Discovery Grant), the Centre for Host−Parasite Interactions at McGill (New Initiatives Grant), and the CRC and CFI Programs. The authors acknowledge G. Faubert (McGill), R. J. Hill (McGill), C. Madramootoo (McGill), and D. G. Brown and Y. Hong (Lehigh) for helpful discussions, S. Gruenheid (McGill) for providing ATCC700927, M. Assanta (AAFC) for providing ATCC43888, and M. Abou-Samra for assistance with bacteria characterization.

Supporting Information Available

Bacteria breakthrough curves measured at 11 °C and cell properties during long acclimation experiments. This material is available free of charge via the Internet at http://pubs.acs.org.

Literature Cited

(1) Smith, J. E.; Perdek, J. M. Assessment and management of watershed microbial contaminants. *Crit. Rev. Environ. Sci. Technol.* **2004**, *34*, 109−139.
(2) Law, D. Virulence factors of *Escherichia coli* O157 and other Shiga toxin producing *Escherichia coli*. *J. Appl. Microbiol.* **2000**, *88*, 729−745.
(3) O'Connor, D. R. Report on the Walkerton Inquiry: Toronto, ON, 2002.
(4) Conboy, M. J.; Goss, M. J. Identification of an assemblage of indicator organisms to assess timing and source of bacterial contamination in groundwater. *Water, Air, Soil Pollut.* **2001**, *129*, 101−118.
(5) Dai, X.; Hozalski, R. M. Evaluation of microspheres as surrogates for *Cryptosporidium parvum* oocysts in filtration experiments. *Environ. Sci. Technol.* **2003**, *37*, 1037−1042.
(6) Hijnen, W. A. M.; Brouwer-Hanzens, A. J.; Charles, K. J. et al. Transport of MS2 phage, *Escherichia coli*, *Clostridium perfringens*, *Cryptosporidium parvum*, and *Giardia intestinalis* in gravel and sandy Soil. *Environ. Sci. Technol.* **2005**, *39*, 7860−7868.
(7) Harvey, R. W.; Harms, H. In *Manual of Environmental Microbiology*, 2nd ed.; Hurst, C. J., Ed.; ASM Press: Washington, DC, 2001; pp 753−776.
(8) Bolster, C. H.; Walker, S. L.; Cook, K. L. Comparison of *Escherichia coli* and *Campylobacter jejuni* transport in saturated porous media. *J. Environ. Qual.* **2006**, *35*, 1018−1025.
(9) Morrow, J. B.; Stratton, R.; Yang, H.-H. et al. Macro- and nanoscale observations of adhesive behavior for several *Escherichia coli* strains (O157:H7 and environmental isolates) on mineral surfaces. *Environ. Sci. Technol.* **2005**, *39*, 6395−6404.
(10) Yang, H.-H. Ph.D. Thesis, The effect of environmental stress on cell surface properties and their relation to microbial adhesion in feedlot *Escherichia coli* isolates. University of Connecticut, Storrs, CT, 2005.
(11) Perna, N. T.; Plunkett, I. G.; Burland, V. et al. Genome sequence of enterohaemorrhagic *Escherichia coli* O157:H7. *Nature* **2001**, *409*, 529−533.
(12) Kenny, B.; Abe, A.; Stein, M. et al. Enteropathogenic *Escherichia coli* protein secretion is induced in response to conditions similar to those in the gastrointestinal tract. *Infect. Immun.* **1997**, *65*, 2606−2612.
(13) Busscher, H. J.; Weerkamp, A. H.; van der Mei, H. C. et al. Measurement of the surface free energy of bacterial cell surfaces and its relevance for adhesion. *Appl. Environ. Microbiol.* **1984**, *48*, 980−983.
(14) Gallardo-Moreno, A. M.; Gonzalez-Martin, M. L.; Bruque, J. M. et al. Influence of the growth medium, suspending liquid, and measurement temperature on the physicochemical surface properties of two enterococci strains. *J. Adhesion Sci. Technol.* **2003**, *17*, 1877−1887.
(15) Hong, Y.; Brown, D. G. Cell surface acid−base properties of *Escherichia coli* and *Bacillus brevis* and variation as a function of growth phase, nitrogen source, and C/N ratio. *Colloids Surf., B* **2006**, *50*, 112−119.
(16) Herbelin, A. L.; Westall, J. C. *FITEQL—A Computer Program for Determination of Chemical Equilibrium Constants from Experimental Data. Report 99-01*; Department of Chemistry, Oregon State University: Corvallis, OR, 1999.
(17) Litton, G. M.; Olson, T. M. Colloid deposition rates on silica bed media and artifacts related to collector surface preparation methods. *Environ. Sci. Technol.* **1993**, *27*, 185−193.
(18) Wilson, W. W.; Wade, M. M.; Holman, S. C. et al. Status of methods for assessing bacterial cell surface charge properties based on ζ potential measurements. *J. Microbiol. Methods* **2001**, *43*, 153−164.

(19) Lytle, D. A.; Johnson, C. H.; Rice, E. W. A systematic comparison of the electrokinetic properties of environmentally important microorganisms in water. *Colloids Surf., B* **2002**, *24*, 91−101.
(20) Lytle, D. A.; Rice, E. W.; Johnson, C. H. et al. Electrophoretic mobilities of *Escherichia coli* O157:H7 and wild-type *Escherichia coli* strains. *Appl. Environ. Microbiol.* **1999**, *65*, 3222−3225.
(21) Pembrey, R. S.; Marshall, K. C.; Schneider, R. P. Cell surface analysis techniques: What do cell preparation protocols do to cell surface properties? *Appl. Environ. Microbiol.* **1999**, *65*, 2877−2894.
(22) Borrok, D.; Turner, B. F.; Fein, J. B. A universal surface complexation framework for modeling proton binding onto bacterial surfaces in geologic setting. *Am. J. Sci.* **2005**, *305*, 826−853.
(23) van der Mei, H. C.; Busscher, H. J. A reference guide to microbial cell surface hydrophobicity based on contact angles. *Colloids Surf., B* **1998**, *11*, 213−221.
(24) Tufenkji, N.; Elimelech, M. Correlation equation for predicting single collector efficiency in physicochemical filtration in saturated porous media. *Environ. Sci. Technol.* **2004**, *38*, 529−536.
(25) Yao, K. M.; Habibian, M. T.; O'Melia, C. R. Water and waste water filtration—Concepts and applications. *Environ. Sci. Technol.* **1971**, *5*, 1105−1112.
(26) Derjaguin, B. V.; Landau, L. D. Theory of the stability of strongly charged lyophobic sols and of the adhesion of strongly charged particles in solutions of electrolytes. *Acta Physicochim. USSR* **1941**, *14*, 733−762.
(27) Verwey, E. J. W.; Overbeek, J. T. G. Theory of the stability of lyophobic colloids. Elsevier: Amsterdam, 1948.
(28) Tufenkji, N. Modeling microbial transport in porous media: Traditional approaches and recent developments. *Adv. Water Resour.* **2007**, *30* 1455−1469.
(29) van Loosdrecht, M. C. M.; Lyklema, J.; Norde, W. et al. The role of bacterial−cell wall hydrophobicity in adhesion. *Appl. Environ. Microbiol.* **1987**, *53*, 1893−1897.
(30) Ryan, J. N.; Elimelech, M. Colloid mobilization and transport in groundwater. *Colloids Surf., A* **1996**, *107*, 1−56.
(31) Abu-Lail, N. I.; Camesano, T. A. The role of lipopolysaccharides in the adhesion, retention, and transport of *Escherichia coli* JM109. *Environ. Sci. Technol.* **2003**, *37*, 2173−2183.
(32) Franchi, A.; O'Melia, C. R. Effects of natural organic matter and solution chemistry on the deposition and reentrainment of colloids in porous media. *Environ. Sci. Technol.* **2003**, *37*, 1122−1129.
(33) Horne, B. D.; Rutherford, E. S.; Wehrly, K. E. Simulating effects of hydrodam alteration on thermal regime and wild steelhead recruitment in a stable-flow Lake Michigan tributary. *River Res. Appl.* **2004**, *20*, 185−203.
(34) Hunter, R. J. Foundations of colloid science. Oxford University Press: New York, 2001.
(35) Garcia-Garcia, S.; Jonsson, M.; Wold, S. Temperature effect on the stability of bentonite colloids in water. *J. Colloid Interface Sci.* **2006**, *298*, 694−705.
(36) Hill, R. J.; Saville, D. A. Exact solutions of the full electrokinetic model for soft spherical colloids: Electrophoretic mobility. *Colloids Surf., A* **2005**, *267*, 31−49.
(37) Greenstein, J. P.; Winitz, M. Chemistry of the amino acids. John Wiley and Sons, Inc.: New York, 1961.
(38) Schwarzenbach, R. P.; Gschwend, P. M.; Imboden, D. M. Environmental organic chemistry. John Wiley and Sons, Inc.: New York, 1993.
(39) Janis, J.; Rouvinen, J.; Leisola, M. et al. Thermostability of endo-1,4-*b*-xylanase II from *Trichoderma reesei* studied by electrospray ionization Fourier-transform ion cyclotron resonance MS, hydrogen/deuterium-exchange reactions, and dynamic light scattering. *Biochem. J.* **2001**, *356*, 453−460.
(40) Yang, S.-T.; Marchio, J. L.; Yen, J.-W. A dynamic light scattering study of β-galactosidase: Environmental effects on protein conformation and enzyme activity. *Biotechnol. Prog.* **1994**, *10*, 525−531.
(41) Drobek, T.; Spencer, N. D.; Heuberger, M. Compressing PEG brushes. *Macromolecules* **2005**, *38*, 5254−5259.
(42) Ouvry, A.; Wache, Y.; Tourdot-Marechal, R. et al. Effects of oxidoreduction potential combined with acetic acid, NaCl, and temperature on the growth, acidification, and membrane properties of *Lactobacillus plantarum*. *FEMS Microbiol. Lett.* **2002**, *214*, 257−261.
(43) Luhm, J.; Schromm, A. B.; Seydel, U. et al. Hypothermia enhances the biological activity of lipopolysaccharide by altering its fluidity state. *Eur. J. Biochem.* **1998**, *256*, 325−333.
(44) Hurme, R.; Rhen, M. Temperature sensing in bacterial gene regulation—What it all boils down to. *Mol. Microbiol.* **1998**, *30*, 1−6.
(45) Gallardo-Moreno, A. M.; Gonzalez-Martin, M. L.; Perez-Giraldo, C. et al. The measurement temperature: An important factor relating to physicochemical and adhesive properties of yeast cells to biomaterials. *J. Colloid Interface Sci.* **2004**, *271*, 351−358.
(46) Walker, S. L.; Redman, J. A.; Elimelech, M. Influence of growth phase on bacterial deposition: Interaction mechanisms in packed-bed column and radial stagnation point flow systems. *Environ. Sci. Technol.* **2005**, *39*, 6405−6411.

Received for review January 20, 2007. Revised manuscript received April 2, 2007. Accepted April 3, 2007.

ES0701558